CONF-810410--1

LA-UR-80-3680

MASTER

TITLE: ELECTRON PROBE MICROANALYSIS IN GEOSCIENCES: A TUTORIAL

AUTHOR(S): Ron Gooley

SUBMITTED TO: Scanning Electron Microscopy/1981
Dallas, TX
April 14 - 18, 1981

University of California

LOS ALAMOS SCIENTIFIC LABORATORY
Post Office Box 1663 Los Alamos, New Mexico 87545
An Affirmative Action/Equal Opportunity Employer

Form No. 836 R3
St. No. 2629
12/78

UNITED STATES
DEPARTMENT OF ENERGY
CONTRACT W-7405-ENG. 36

ELECTRON PROBE MICROANALYSIS IN GEOSCIENCES: A TUTORIAL

Ron Gooley

Geosciences Division

Los Alamos Scientific Laboratory

Los Alamos, New Mexico 87544

I. INTRODUCTION

The technique of x-ray spectrochemical analysis has resulted from Moseley's[1] discovery that the wavelength (or energy) of emitted x radiation is a function of atomic number, and is characteristic of the emitting element. Applications of this technique were pursued through the 1920's and 1930's; most notable was the discovery and identification of hafnium from its x-ray wavelengths by Coster and von Hevesy.[2] In the late 1940's, while electron microscopy was developing rapidly, a patent was issued to J. Hillier[3] that described the concept of electron probe microanalysis (EPM). However, Hillier did not pursue the concept. At the 1949 Electron Microscope Conference in Delft, Netherlands, Castaing and Guinier[4] presented their first report describing specimen excitation by an electrostatically focussed electron beam, and measurement of characteristic emitted x radiation by an x-ray spectrometer. Castaing subsequently improved the instrument by introducing electromagnetic beam focussing lenses in place of the electrostatic lenses. In his brilliant doctoral thesis,[5] he discussed relationships between specimen composition and x-ray intensity, and formulated the basis for many current data reduction algorithms.

Geoscientists were slow to begin using the instrument; by 1964, only 60 geoscience papers had been published using EPM data.[6] Since that time, the

instrument has revolutionized petrology and geochemistry. Almost all major geoscience departments in academic, industrial and governmental laboratories now use the EPM extensively, and papers dealing with EPM use in the geosciences now number in thousands. In addition to its extensive application to a wide variety of mineralogical and petrological problems, the EPM recently has been applied in organic geochemistry, primarily for characterizing the occurrence of organic sulfur in coal.

It is probably justifiable to say that advances in modern electronics and computer technology have revolutionized the EPM as much as the EPM has affected the geosciences. A complete description of these achievements is beyond the scope of this tutorial paper, but it is important to gain some appreciation of the sophistication of modern instruments. Consider that about five or six years ago a minicomputer with 16K bytes of memory cost about $30K; one with 256K bytes is now about $20K.

Minicomputers are now capable of controlling beam current, detector voltages, pulse-height analyzer baseline and window values, wavelength-dispersive spectrometer movement, and sample stage motion in X, Y, and Z directions while simultaneously handling highly sophisticated data reduction algorithms on line. In some instruments, microprocessors that interact with a minicomputer replace counter/timers and ratemeters for data collection, and axis positioners for spectrometer and sample stage control. Condenser and objective lens parameters are automatically adjusted by microprocessors for proper electron beam control as the operator changes or selects accelerating voltage or beam current for a particular task.

Although these advances in technology have not significantly broadened the range of application of electron microanalysis, they have enabled much more rapid analyses, and have greatly reduced chances for operator error.

In addition, they have enabled manufacturers to hold prices relatively stable during a long period of spiraling inflation.

II. THE ELECTRON PROBE MICROANALYZER

The EPM uses a finely focussed electron beam which produces x rays characteristic for elements present in the sample. The electron column and basic instrumentation of the EPM are very similar to those of a scanning electron microscope (SEM). The major difference between the two instruments and their modes of operation, is that in general, the EPM is used to determine chemical composition, while the SEM defines surface morphology of the specimen, i.e., produces a magnified image of the specimen.

Both instruments use a finely focussed electron beam which impinges on the sample with accelerating voltage generally at 15 or 20 keV. Most modern EPMs can function in a SEM mode, and some SEMs, when equipped with x-ray spectrometers, are virtually the same as EPMs. In fact, modern electron beam instruments are so versatile that the distinction between an EPM and a SEM becomes rather vague. For the purposes of this discussion, I shall define an EPM as an electron beam instrument that uses wavelength dispersive spectrometers (WDS) for x-ray analysis and an optical microscope for specimen viewing during analysis. Modern SEMs are commonly equipped with energy dispersive spectrometers (EDS) to permit chemical analysis. Until recently, EDS was limited to qualitative analysis (i.e., identifying only what elements are present, but not quantitative composition). In the last three or four years, significant progress has been made, and several manufacturers now offer quantitative data reduction software for EDS systems that produces results approaching those of WDS analysis.

A. Electron Column

Figure 1 shows a schematic representation of the basic components of an EPM. The electron gun is of triode design, with a tungsten filament, a grid cylinder and an anode. Thermionic emission from the heated filament is the source of free electrons. The electrons are accelerated down the column through a hole in the anode, which operates at a high positive potential (generally 15 or 20 keV) with respect to the filament. The grid, or Wehnelt cup, which is operated at a negative potential with respect to the filament, controls emitted current. Commonly, a feedback circuit from a beam limiting aperture lower in the columnn adjusts the grid bias to regulate beam current. The grid also actually forms an electrostatic lens and decreases the beam diameter.

The beam is further shaped and demagnified by apertures and electromagnetic lenses. Older EPMs commonly used one condenser lens and one final probe-forming (objective) lens; most SEMs and more modern EPMs generally use two condenser lenses and the final lens. The electron beam is focused to a diameter of about 1 μm for EPM use; beam diameter for SEM use may be as small as 50 Å. The EPM beam also may be defocused or rastered at the point of sample impingement to perhaps as much as 50 μm across, i.e., the spot size or rastered area of analysis is enlarged. This practice is especially common with beam-sensitive samples, or when it is desirable to obtain an "averaged" analysis over a broader area if the sample is compositionally inhomogeneous on a micrometer-size scale. With WDS work, caution must be exercised with "broad beam" analysis to be certain that the spectrometers are in x-ray focus across the entire width of the beam. Energy dispersive detectors "see" a much larger sample area than wavelength dispersive spectrometers, so this potential problem is not as critical.

B. Wavelength Dispersive Spectrometry (WDS)

Excellent wavelength resolution, high peak to background intensity ratios, low detection limit (<0.01% for many elements), and the ability to analyze x-rays emitted from low Z elements (B, C, N, O) are the prime merits of WDS. These spectrometers employ a curved crystal which is mechanically moved to diffract x-rays into a gas proportional detector at positions where Bragg's law is satisfied:

$$N\lambda = 2 d \sin \theta \qquad (1)$$

where N is an integer, λ is the x-ray wavelength, d is the crystal lattice spacing, and θ is the angle of x-ray incidence on the crystal. The wavelength range for which a particular crystal is suitable is limited, and is dependent on its d spacing. A variety of crystals are available to cover all elements from Z = 5 (B) to Z = 92 (U). Perhaps the most common crystals now used in modern EPMs are LiF (Lithium Fluoride), PET (Pentaerythritol), TAP (Thallium Acid Phthalate), and ODPb (Lead Orthodecate), the latter for B, C, N and O.

Detector output pulses are shaped, amplified, digitized, and (on automated instruments) stored on computer for on-line data reduction. Most EPMs are equipped with multiple spectrometers, each with a different crystal. For example, on an instrument with three spectrometers, one might use a TAP crystal on one spectrometer, a PET on the second, and a LiF crystal on the third. Spectrometers are commonly equipped with automated crystal changers. On automated instruments, each spectrometer is computer-driven to the peak position for each selected element within its wavelength range and to a preselected position off of each peak for background determination. Peak and/or background intensities are determined at each position by a preselected counting time or number of counts. After

x-ray intensities are determined on the analytical standards, a typical 10-element analysis takes approximately two minutes using an efficient automation-data reduction software system.

Figure 1 schematically shows positioning of the sample, crystal and detector on the Rowland circle. Mechanisms for moving the crystal and detector as the spectrometer is scanned through its wavelength range are fairly complex and must be well engineered. The sample, crystal and detector must always remain on the Rowland circle, and the x-ray take-off angle must remain constant.

C. Energy Dispersive Spectrometry (EDS)

Energy dispersive x-ray spectrometry makes use of a semiconductor (solid state) x-ray energy detector and multichannel analyzer (MCA) for energy analysis. X-ray photons impinging on a litnium drifted silicon (SiLi) semiconductor detector create electron-hole pairs. (A "hole" is a lattice site that carries an effective positive charge by the loss of an electron that is promoted to a higher energy level, the conduction band shared by the entire crystal). When a potential is applied across the crystal in its ground state, little or no current flows, but x-ray photon absorption creates an amount of "free" charge that reflects the energy of the incident photon. The applied potential carries the charge (electrons and holes) to a charge-sensitive preamplifier which converts the charge pulse to a voltage pulse. The voltage pulse is amplified, shaped, and passed to a multi-channel analyzer. The basis for energy spectroscopy is the relationship between charge and absorbed x-ray photon energy.

The MCA sorts the incoming signal according to variations in pulse amplitude (corresponding to variations in photon energy). It counts and

stores in memory the number of pulses that fall into channels (pulse amplitude windows) and displays the resulting energy spectrum on a catnode-ray tube. Most modern MCA systems provide at least 1024 channels and have a selective operational range (e.g., 0-10 keV, 0-20 keV, 0-40 keV, etc.). For 1024 channels and an operating range of 0-10 keV, each channel covers ~10 eV. Some type of cursor, or channel marker, which can be electronically moved to a selected channel is displayed on the CRT, as is the number of the selected channel. It is convenient with inexpensive MCAs to operate with 1024 channels at 0-10 keV full range, because when the cursor is moved to an x-ray peak, the channel number corresponds (with proper placement of a decimal point) to the x-ray line energy. For example, the energy of the Si Kα line is 1.787 keV, and the channel number will read 179. More sophisticated MCAs commonly are programmed to display the element symbol, the x-ray line, and other pertinent information.

D. Light Optics

A light optical microscope allows for specimen viewing at high magnification to accurately position the electron beam on the area of interest. For proper x-ray focusing into the detector, the sample, diffracting crystal, and detector must lie on the perimeter of the Rowland circle at all times during analysis. The focal point of the microscope is coincident with the focal point of the crystal spectrometer to assure correct sample positioning for x-ray focus.

III. ELECTRON BEAM-SAMPLE INTERACTIONS

When the electron beam impinges on a sample, several things happen (Figure 2), a few of which are pertinent to the present discussion. Electrons penetrate below the sample surface (about 1 to 3 μm at 15 keV, depending on sample composition and structure) and undergo a series of

elastic and inelastic interactions with electrons of sample atoms. Some inner shell sample electrons are ejected; this process is followed by outer shell electrons cascading in to fill the vacancies. The energy difference between the inner shell (vacancy) and the outer shell (original site of the transposed electron) is manifested by emission of a photon. Electron energy levels are discrete and characteristic for each element. Therefore emitted x-rays are characteristic in energy (or wavelength) for each element in the sample, neglecting the background white spectrum present due to the large number of electron interactions. This is the basis for x-ray analysis.

Some electrons are elastically backscattered and are lost for x-ray production; these must be considered during x-ray data reduction. Other beam electrons undergo inelastic collisions, ejecting sample electrons and losing some energy to them. Some ejected sample electrons (secondary electrons) have low energy (typically <50 eV) and are easily reabsorbed by the sample. Some secondary electrons produced very near the surface escape; these are utilized for imaging in the SEM.

The relationship between the abundance ratio of the unknown and standard for element A and the ratio of x-ray intensities emitted from the unknown and standard by element A is given by:

$$\frac{C_U^A}{C_S^A} = \frac{I_U^A}{I_S^A} \text{ ; therefore: } C_U^A = \frac{I_U^A}{I_S^A} \cdot C_S^A \qquad (2)$$

where C is concentration, I is x-ray intensity, U and S denote unknown and standard, and A implies element A. However, this relationship is valid if and only if the unknown and standard are identical in composition and

structure. Observed x-ray intensity is affected by specimen absorption, secondary x-ray fluorescence, electron backscattering and electron stopping power. All of these factors are functions of sample composition and structure, and are commonly referred to as matrix or ZAF effects (Z = atomic number, A = absorption, F = fluorescence). Data reduction algorithms calculate and correct for these effects.

A. Atomic Number Effect

Sample composition and structure affect electron interactions, and therefore x-ray production, in the sample in two ways: electron backscatter and electron stopping power. Both of these factors increase with increasing electron density of the sample, or with increasing average atomic number Z. Backscattered electrons result from single and multiple elastic interactions between incident (beam) and sample electrons and are lost to x-ray production. Castaing[7] obtained an expression to describe electron penetration (therefore stopping power) into a sample:

$$\rho R(x) = 0.033 \, (E_0^{1.7} - E_c^{1.7}) \, A/Z$$

where ρ is sample density in g/cm^3, R(x) is distance in μm, and E and E_c, both in keV, are electron beam energy and the critical excitation potential of the target, below which no x-ray production can occur. Others have revised and tested this equation experimentally; a brief review is given by Goldstein.[8] Electron penetration for x-ray production into common silicate minerals at 15 keV accelerating potential is less than 2 μm; into a low-Z material such as coal it would be less than 4 μm.

B. Absorption

As depicted in Figure 2, most x-ray production occurs beneath the sample surface. As x-rays pass through sample materials, some are absorbed

and x-ray intensity seen by the detector is reduced with respect to primary x-ray production in the sample. The amount of absorption that occurs is dependent on sample composition and the pathlength through the sample, which in turn is proportional to the cosecant of the x-ray take-off angle (ϕ in Figure 2). It follows then, that absorption is greater with instruments employing a low x-ray take-off angle.

C. Fluorescence

Characteristic x radiation produced by electron excitation of sample atoms can excite other sample atoms, producing a secondary fluorescence effect. This phenomenon has the opposite effect of absorption and may cause observed radiation for some elements to be enhanced. Generally, x-ray absorption affects observed intensity to a greater degree than fluorescence, but the opposite may happen in compounds or alloys where two elements close in atomic number are present. For example, consider an Fe-Ni alloy with equal amounts of each element. Fluorescence of Fe Kα radiation by Ni Kα radiation dominates over absorption, and Ni Kα radiation is strongly absorbed by Fe. As absorption decreases with increasingly higher x-ray take-off angle, fluorescence becomes increasingly important.

D. Instrumental Effects

Data reduction must also consider background counts, instrumental drift, and detector deadtime. These factors are commonly called instrumental effects. Background arises from two sources: 1) stray pulses or signals due to electronic noise, and 2) the x-ray continuum due to the almost infinite variety of electron-electron and electron-photon interactions. Small changes may occur in electron beam intensity between standard and sample x-ray intensity measurements due to variations in the instrument's electronics. Therefore beam current is commonly monitored,

and x-ray intensities are adjusted by a normalization factor whenever this drift is significant. Most wavelength dispersive x-ray detectors employ gas proportional counters. These devices have a finite pulse resolving time, commonly on the order of 2 microseconds, which produces a non-linear response at high counting rates. Thus a correction facotr for this detector "deadtime" must be applied, especially when there are significant differences in contents of the element of interest between sample and standard.

E. Data Reduction

Reduction of raw x-ray intensity data to meaningful composition data is now almost always done by computer. Modern EPMs generally use a dedicated minicomputer for on-line data reduction and instrument automation. Beaman and Isasi[9] critically reviewed available data reduction programs in 1970. Basic techniques in data reduction algoritnms have changed little since that time, but considerable progress has been made in combined automation-data reduction schemes and also in faster, more efficient software routines. A prospective EPM buyer should investigate the field thoroughly before purchase.

IV. STANDARDS AND SAMPLES

A. Analytical Standards

Quantitative analysis by EPM is conducted by comparing the x-ray intensity produced from a sample to that produced on a standard of known composition. Therefore, standard quality is of utmost importance in producing acceptable quantitative data. Acquiring good standards is a particular problem in geosciences due to compositional complexity and inhomogeneity of most minerals. Observed x-ray intensities (those "seen" by the spectrometers) differ from the intensities of x-rays actually

generated by electron bombardment of the specimen because of the x-ray absorption, fluorescence, and atomic number effects. These effects depend directly on specimen composition, thus the ideal standard is one whose composition is identical to the unknown. Complete sets of well-analyzed, homogeneous mineral standards, either natural or synthetic, spanning large compositional ranges, are not available. The analyst, therefore, generally must resort to a standard that is hopefully close in composition to the specimen. The very nature of microanalysis places serious restrictions on standards:

1. Its composition must be accurately known.
2. It must be compositionally homogeneous on a sub-micron scale.
3. It must be stable under vacuum, in air, and under electron bombardment.
4. It must be in a form that can be polished to expose a flat, crack-free surface.

There are relatively few natural minerals that satisfy the above criteria and are available in sufficient quantity to enable accurate, independent chemical analysis, with enough remaining for distribution to the "EPM community". Considerable effort is required to prepare a standard for EPM use:

1. Polished sections (for opaque material) or petrographic thin sections (for translucent phases) are prepared and studied microscopically in reflected and transmitted light for undesirable features such as foreign phases, chemical zoning, exsolution lamellae, etc.

2. The material is thoroughly tested for homogeneity by EPM; EPM analyses should be conducted for all elements at points as far apart as possible and at the extreme edges of the material.
3. An independent, complete chemical analysis is then obtained by a competent, trusted analyst or analysts (preferably two or three) on a split of the material.
4. Before distribution, the chemical analysis should be checked by EPM against several known standards. (A wise researcher will also do this with each new standard he/she obtains).

Most laboratories accumulate a large collection of standards with time, but few are available in sufficient quantity for broad distribution between many laboratories. Therefore, unfortunately, very little inter-laboratory calibration has occurred.

B. Samples

Types of samples used for EPM analysis are commonly the same as for optical microscopy. Standard polished sections like those used in metallurgy, or polished petrographic thin sections (with no cover slip) are the most common samples. It is very important to prepare well polished, flat samples, i.e., as free of scratches and surface relief as possible. X-ray production by electron beam excitation occurs within approximately 2 μm of the sample surface. The intensity of x-rays emerging from beneath the surface is dependent upon their pathlength through sample materials. The x-ray path length out of the sample is increased considerably if the electron beam is positioned in the bottom of a scratch on the sample surface (Fig. 3), thus greatly increasing absorption of the emerging x-rays, especially for those of light elements. Long[10] reported that the observed x-ray intensity for Mg in a pyroxene of composition $En_{50}Fs_{50}$ is

reduced approximately 10% when an electron beam with accelerating voltage of 15 kV is positioned in a 0.5 μm deep scratch in an instrument with a 20° take-off angle. Naturally, this error is minimized with higher take-off angle.

In addition to avoiding surface scratches, it is important to maintain a flat, relief-free surface during sample polishing. The sample and standard(s) should be positioned in the instrument such that the surfaces of both are in a fixed plane, with the x-ray take-off angle being the same as that used for calculation of absorption correction.[10,11] An appreciable difference in x-ray absorption may result from a moderately small change in specimen tilt. Sweatman and Long[12] reported the error in Mg determination in an olivine as a function of angle of specimen tilt for a series of instrument take-off angles (Fig. 4).

Most geologic materials are poor electrical conductors. Therefore, to prevent charge build-up on the sample surface at the point of electron impact and resulting beam deflection, the sample must be coated by a thin layer of conductive material before analysis. A vacuum evaporator is used to deposit the conductive layer. For several reasons carbon is generally used instead of materials such as Be, Al, Cu, Au, etc. In thin film, carbon is optically transparent, facilitating specimen viewing during analysis. Carbon is non-poisonous (the problem with BeO), does not appreciably absorb electrons or soft x-rays (the problem with Au or Cu), and except for carbonate minerals, is generally not an element of interest in geological samples (Al commonly is).

Most geological materials are poor thermal conductors. This means that heat generated under an intense electron beam may seriously affect some samples by vaporizing volatile sample material, especially in samples such

as oil shale or some coals. Vaporization of water from strongly hydrated samples may lift or tear the carbon thin film and affect conduction. Thermal problems can be reduced by defocusing the electron beam to produce a large spot size, operating in a beam raster mode, or lowering beam intensity by reducing accelerating voltage and/or beam current. A related potential problem is Na migration away from the electron beam. Migration is apparently due to the "electron-phobic" nature of Na, and is more problematic in glasses than in crystalline materials.

V. APPLICATIONS

Keil[6] published a nice review of applications of the EPM in geosciences. Most involve chemical analyses of common major and minor mineral-forming elements for a wide variety of mineralogical/petrological problems. Present high rates of publication prohibit any attempt at a complete review, nor would it serve a useful purpose. Instead, I will briefly describe some recent applications.

Luth, Chambers and Gerlach[13,14] used an automated EPM for determination of modal abundance and chemical composition of phases in basalt samples from the Kilauea Iki (1959) Lava Lake. Their automation system controls beam current, detector voltages, spectrometers and stage motion using software developed by Chambers.[15,16,17,18] They conducted 300-400 analyses for 12 elements on each of 30 samples obtained from three drill holes penetrating about 63 meters into the lava lake. They were able to define four "magmatic" zones in this distance. Their analyses were conducted at night, in the absence of an operator, with the instrument under computer control. This application demonstrates the power of a fully automated system.

Brown and Mullins[19] reported EPM results for whole rock analysis using 20 milligram samples. Their technique involves fusing into glass a representative sample of a rock powder on a metallic strip heater under argon atmosphere. This technique is especially useful when only small sample amounts are available, e.g., for lunar samples of 100 mg allocation. They ran a suite of basalts from Leg 34, Deep Sea Drilling Project. Their results, compared with x-ray fluorescence and neutron activation values, were well within acceptable limits for EPM. However, the technique is not equally applicable to all rocks. In Mg-rich rocks such as peridotites, olivine crystals form with interstitial glass even with rapid quenching. Glasses prepared from rocks rich in SiO_2 such as rhyolites or granites tend to be heterogeneous. They report that "when the technique is applied to rocks of limited composition range, high quality major element analyses can be produced."

One application of EPM in our laboratory concerns occurrence and distribution of organic sulfur in coal. Direct determination of organic sulfur by EPM provides a rapid method that eliminates the uncertainties inherit in conventional ASTM methods of calculating organic sulfur by difference.[20] Microanalysis of individual coal macerals has shown a consistent trend for organic sulfur contents: sporinite, resinite, micrinite, and resinite > pseudovitrinite $\geq$ macrinite $\geq$ semifusinite > fusinite.[21] Furthermore, EPM results have shown correlations between optical reflectance (in oil) and organic sulfur contents of various macerals,[22] and how depositional environments of peat alter the sulfur content of the eventual coal.[23]

ACKNOWLEDGMENT

Portions of this paper were taken from a previous publication.[24] I am grateful to Academic Press, Inc. for allowing this privilege. This work is supported by the Department of Energy, Division of Basic Energy Sciences.

REFERENCES

1. Moseley, H. (1913). "The High-Frequency Spectra of the Elements I," Philos. Mag. 26, 1024-1034.
2. Coster, D., and von Hevesy, G. (1923). "The New Element Hafnium," Naturwissenchaften 11, 133.
3. Hillier, J. (1947). U.S. pat. No. 2, 418,029.
4. Castaing, R., and Guinier, A. (1949). "Application des Sondes Electroniques à l'Analyse Métallographique," in "Proc. Intern. Conf. Electron Microscopy, Delft, 1949." Nijhoff, The Hague, 60-63.
5. Castaing, R. (1951). "Application des Sondes Electroniques à une Méthode d'Analyse Ponctuelle Chimique et Cristallographique," Ph.D. Thesis, Univ. of Paris, 140 pp.
6. Keil, K. (1973). "Application of the Electron Microprobe in Geology," in "Microprobe Analysis" (C. A. Anderson, ed.), Wiley (Interscience), New York, 189-239.
7. Castaing, R. (1960). "Electron Probe Microanalysis," Adv. Electron. Electron Phys. 13, 317-386.
8. Goldstein, J. I. (1975). "Electron Beam-Specimen Interactions," in "Practical Scanning Electron Microscopy" (J. I. Goldstein and H. Yakowitz, ed's.) Plenum Press, New York, 49-94.

9. Beaman, D. R., and Isasi, J. A. (1970). "A Critical Examination of Computer Programs Used in Quantitative Electron Microprobe Analysis," Anal. Chem. 42, 1540-1568.

10. Long, J. V. P. (1967). "Electron Probe Microanalysis," in "Physical Methods in Determinative Mineralogy" (J. Zussman, ed.), Academic Press, 215-260.

11. Yakowitz, H., and Heinrich, K. F. J. (1968). "Quantitative Electron Probe Microanalysis: Absorption Correction Uncertainty," Microchim. Acta, 182-200.

12. Sweatman, T. R., and Long, J. V. P. (1969). "Quantitative Electron-Probe Microanalysis of Rock-Forming Minerals," J. Petrol. 10, 332-379.

13. Chambers, W. F., and Luth, W. C. (1980). "Automated Modal and Mineralogical Analyses Using the Electron Microprobe: Kilauea Iki (1959) Lava Lake," Abstr. accepted for Fall Meeting, AGU, San Francisco.

14. Luth, W. C., and Gerlach, T. M. (1980). "Compositions and Proportions of Major Phases in the 1959 Kilauea Iki Lava Lake in December 1978," Abstr. accepted for Fall Meeting, AGU, San Francisco.

15. Chambers, W. F. (1978). "Sandia-Task '78: An Electron Microprobe Automation Program," SAND78-1149, Sandia Laboratories, Albuquerque, NM.

16. Chambers, W. F. (1979). "BA78: An Improved Bence-Albee Analysis Program for Tracor Northern Systems," SAND78-1835, Sandia Laboratories, Albuquerque, NM.

17. Chambers, W. F. (1979). "QUANT: A Quantitative Analysis Schedule for Tracor Northern Automated Electron Microprobes," SAND78-1836, Sandia Laboratories, Albuquerque, NM.

18. Chambers, W. F. (1979). "SETUP: An Auxiliary Program for Establishing Measurement Parameters for Quantitative Microprobe Analyses," SAND78-2263, Sandia Laboratories, Albuquerque, NM.

19. Brown, R., and Mullins, O., Jr. (1975). "Electron Microprobe Whole Rock Analysis of 20 mg Samples," Proc. Microbeam Analysis Soc., pp. 32A-32D.

20. Raymond, R., Jr., and Gooley, R. (1978). "A Review of Organic Sulfur Analysis in Coal and a New Procedure," Scanning Electron Microsc. 1978 1, 93-108.

21. Raymond, R., Jr. (1979). "Relative Abundances of Common Elements in Coal Macerals," in "Microbeam Analysis - 1979" (D. Newbury, ed.), San Francisco Press, 105-109.

22. Raymond, R., Jr., and Davies, T. D. (1981). "Organic Sulfur in Coal: Relationsnip to Macerals, Rank, and Depositional Environments," Abstr. submitted to Amer. Chem. Soc. Mtg., Atlanta, GA.

23. Raymond, R., Jr. (1979). "Content and Form of Sulfur in Coal: A Reflection of peat Depositional Environments," GSA Abstracts, p. 501.

24. Raymond, R., Jr., and Gooley, R. (1979). "Electron Probe Microanalyzer in Coal Research," in "Analytical Methods for Coal and Coal products, Vol. III" (Clarence Karr, Jr., ed.), Academic press, 337-356.

FIGURE CAPTIONS

Fig. 1. Schematic representation of the EPM showing the electron column configuration and placement of the sample, curved crystal and gas detector on the Rowland circle. (After Raymond and Gooley[24]).

Fig. 2. Representation of electron beam impingement on a sample, resulting in generation of x rays, backscattered electrons, and secondary electrons. The volume of sample energized to produce x rays is much larger than suggested by the small area defined by beam impingement on the sample. The x ray take-off angle is shown by ϕ. (After Raymond and Gooley[24]).

Fig. 3. Representation of electron beam placement in a scratch. Note the additional path length for x-ray travel through sample material. (After Long[10]).

Fig. 4. Plot of error in Mg determination as a function of specimen tilt ($\Delta\theta$) for a series of instrumental take-off angles. (After Sweatman and Long[12]).

Fig. 1

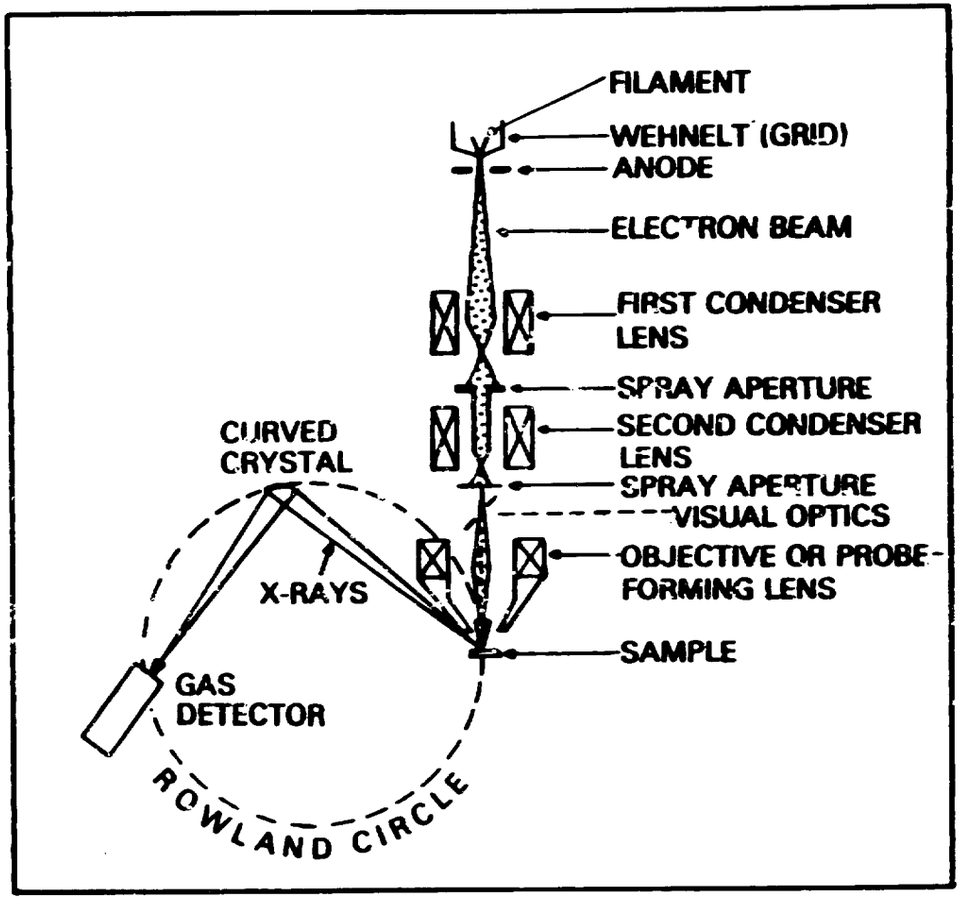
FILAMENT
WEHNELT (GRID)
ANODE
ELECTRON BEAM
FIRST CONDENSER LENS
SPRAY APERTURE
SECOND CONDENSER LENS
SPRAY APERTURE
VISUAL OPTICS
OBJECTIVE OR PROBE FORMING LENS
SAMPLE
CURVED CRYSTAL
X-RAYS
GAS DETECTOR
ROWLAND CIRCLE

Fig. 2

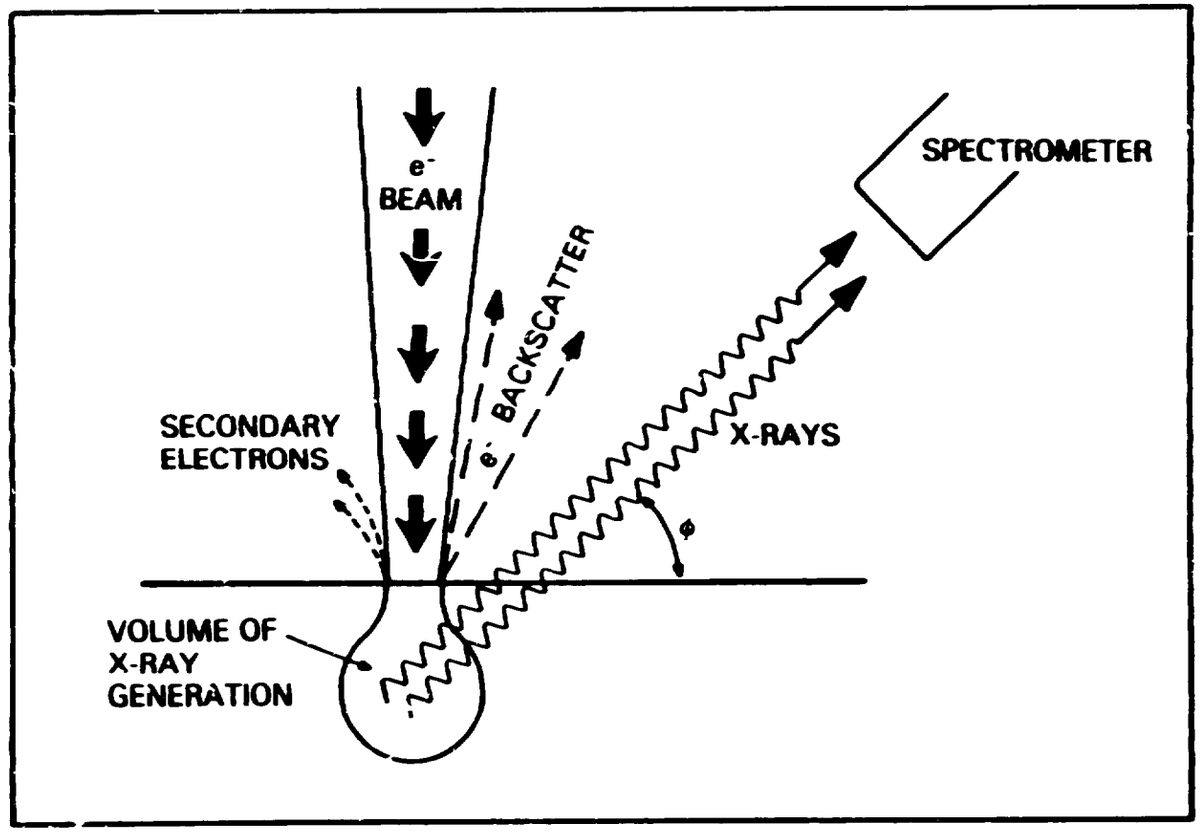
e⁻
BEAM
SPECTROMETER
e⁻ BACKSCATTER
SECONDARY
ELECTRONS
X-RAYS
φ
VOLUME OF
X-RAY
GENERATION

Fig 3

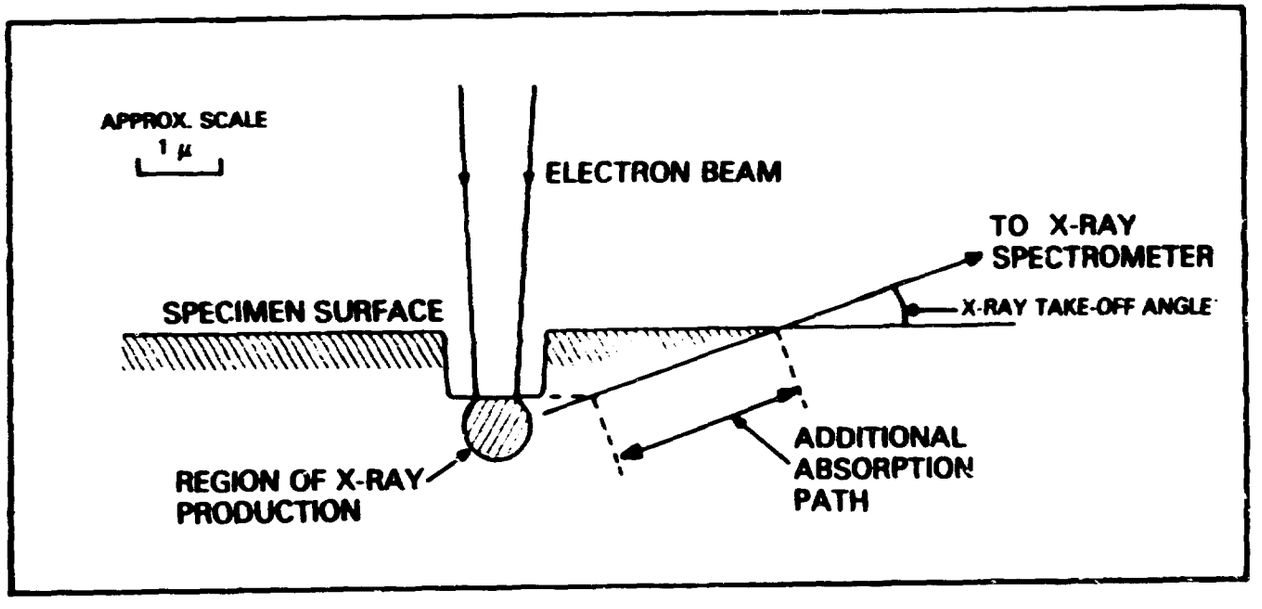
APPROX. SCALE
1 μ
ELECTRON BEAM
TO X-RAY SPECTROMETER
X-RAY TAKE-OFF ANGLE
SPECIMEN SURFACE
ADDITIONAL ABSORPTION PATH
REGION OF X-RAY PRODUCTION

Fig 1

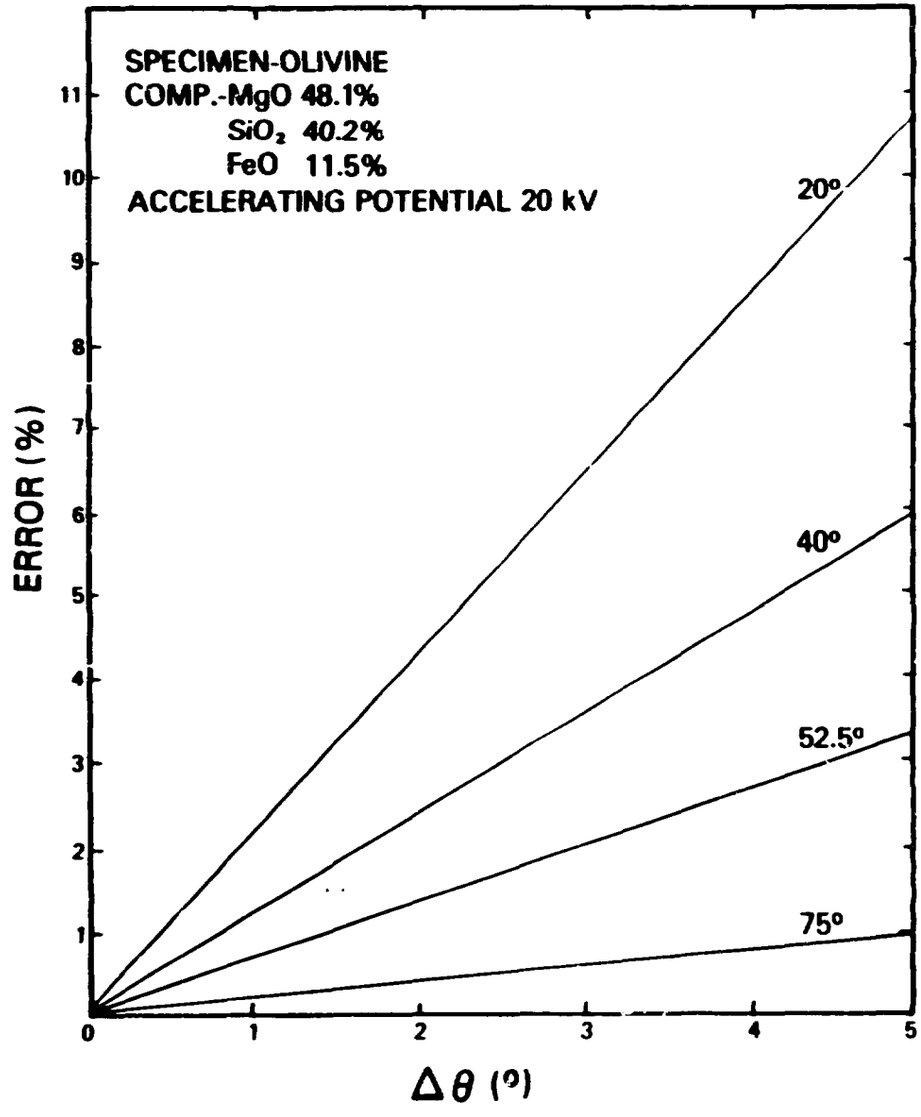
SPECIMEN-OLIVINE
COMP.-MgO 48.1%
SiO2 40.2%
FeO 11.5%
ACCELERATING POTENTIAL 20 kV
20°
40°
52.5°
75°
ERROR (%)
Δθ (°)
0
1
2
3
4
5
1
2
3
4
5
6
7
8
9
10
11